Supporting Information

A chemodosimetric approach for visual detection of nerve agent simulant diethyl chlorophosphate (DCP) in liquid and vapour phase

Atanu Maji, Amitav Biswas, Biswajit Bera and Tapan K. Mondal*

Department of Chemistry, Jadavpur University, Kolkata- 700032, India. E-mail:tapank.mondal@jadavpuruniversity.in

CONTENTS

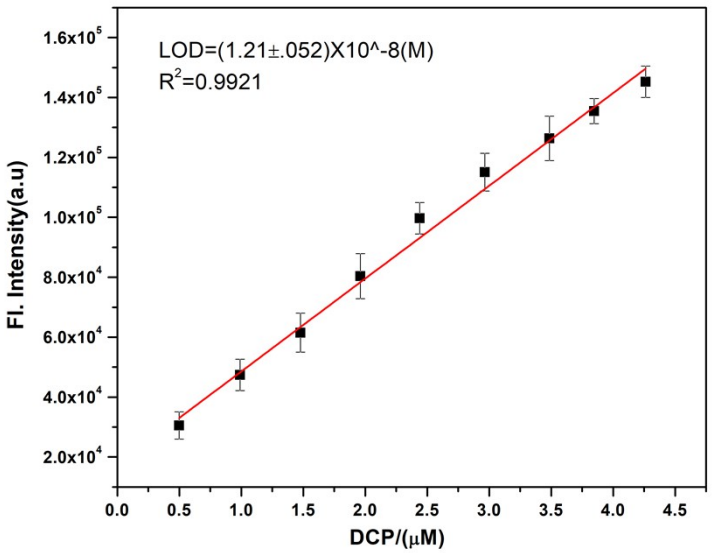

Fig. S1. Linear response curve of BIPQ at 468 nm depending on the DCP concentration

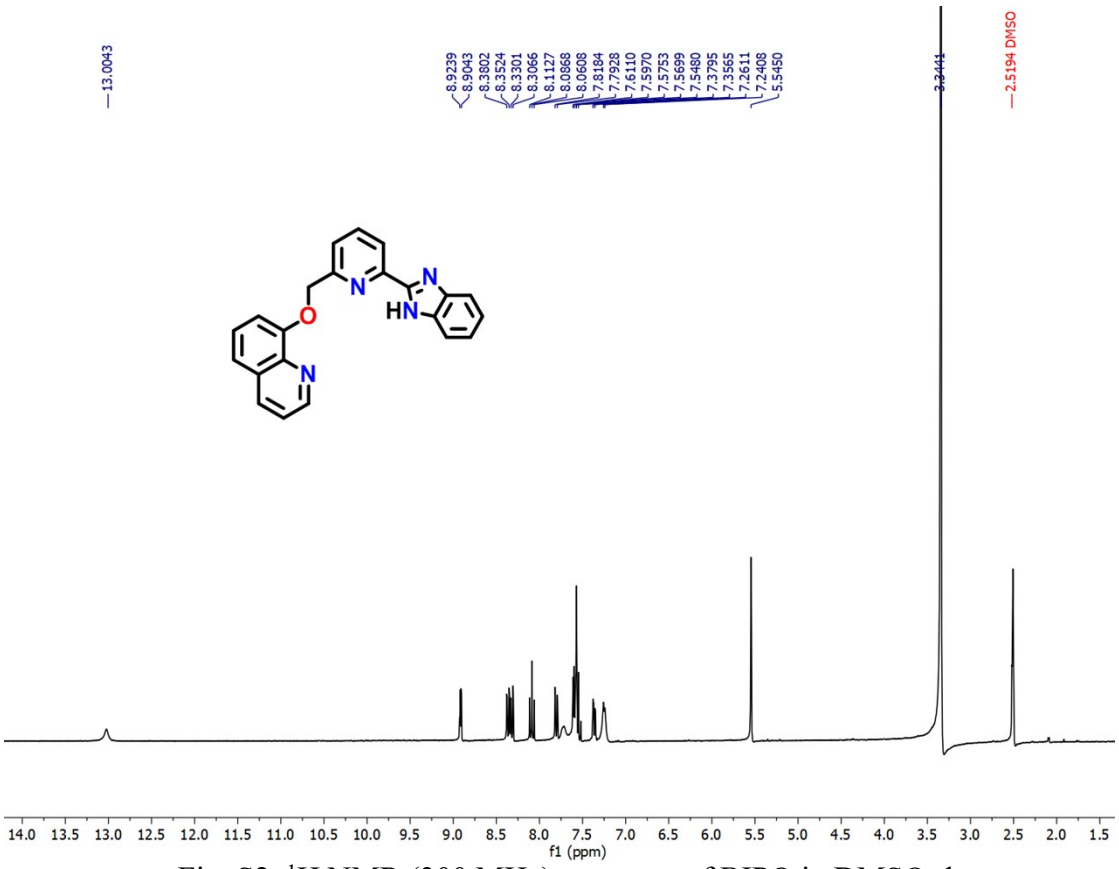

Fig. S2. ^{1}H NMR (300 MHz) spectrum of BIPQ in DMSO-d_6

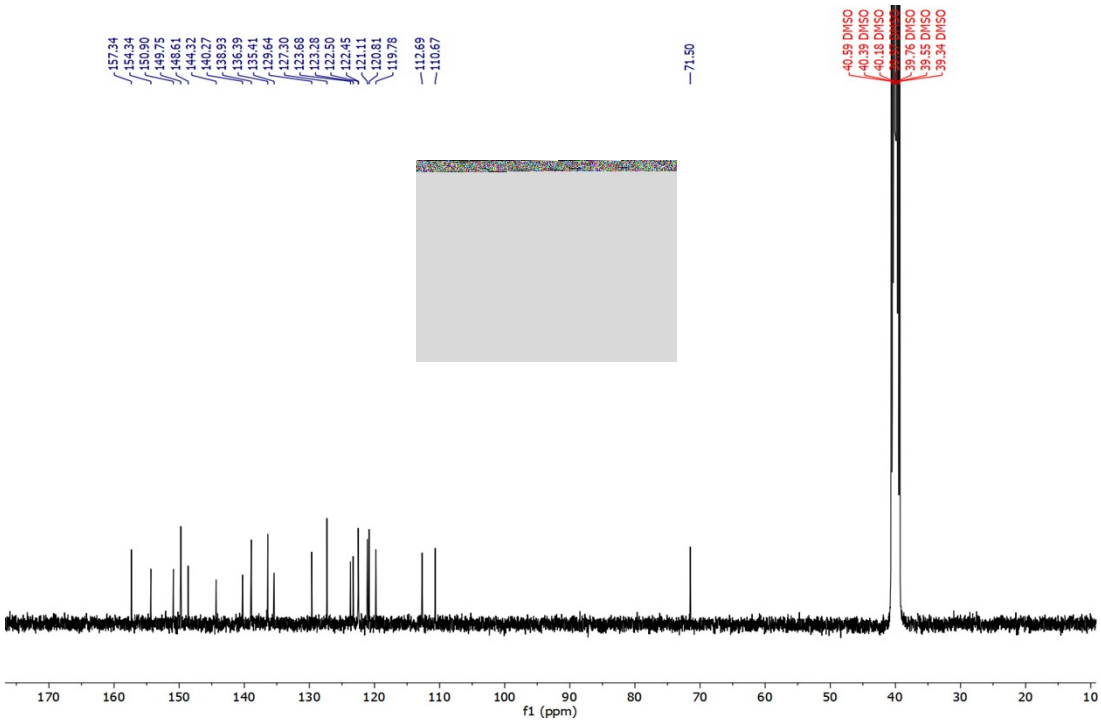

Fig. S3: ^{13}C NMR (75 MHz) spectrum of BIPQ in DMSO-d_6

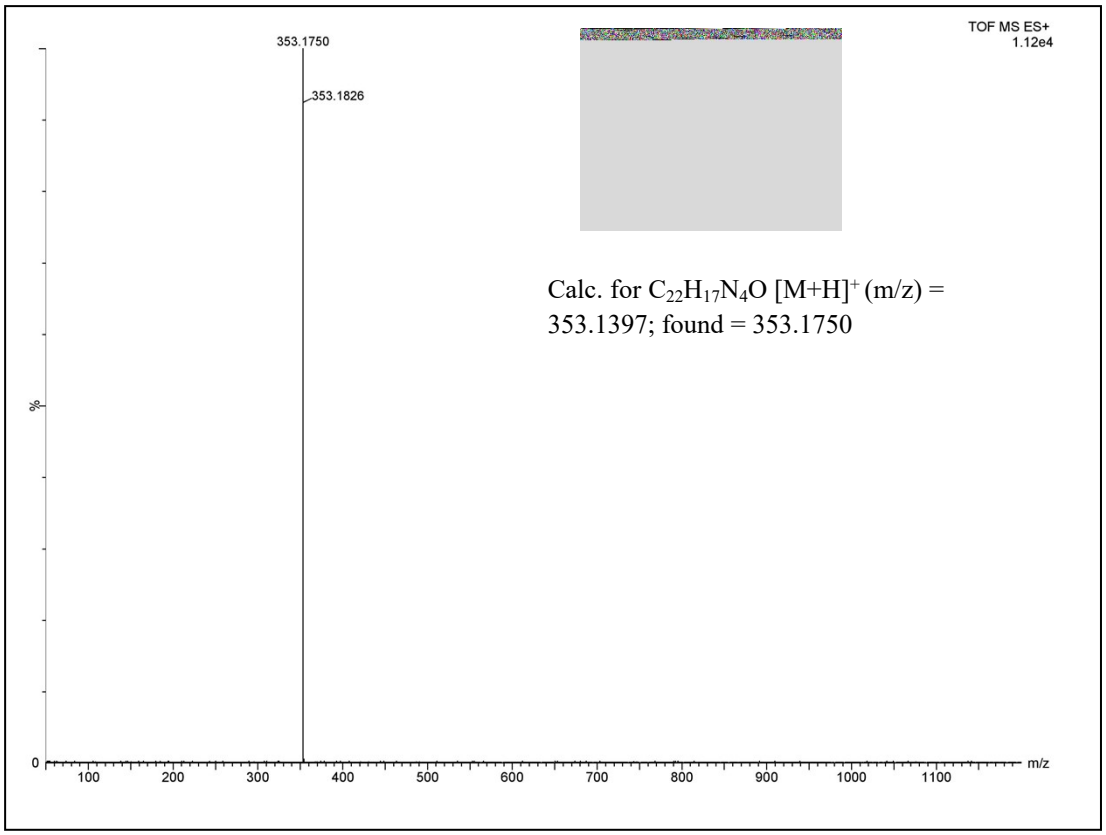

Fig. S4. HRMS of BIPQ

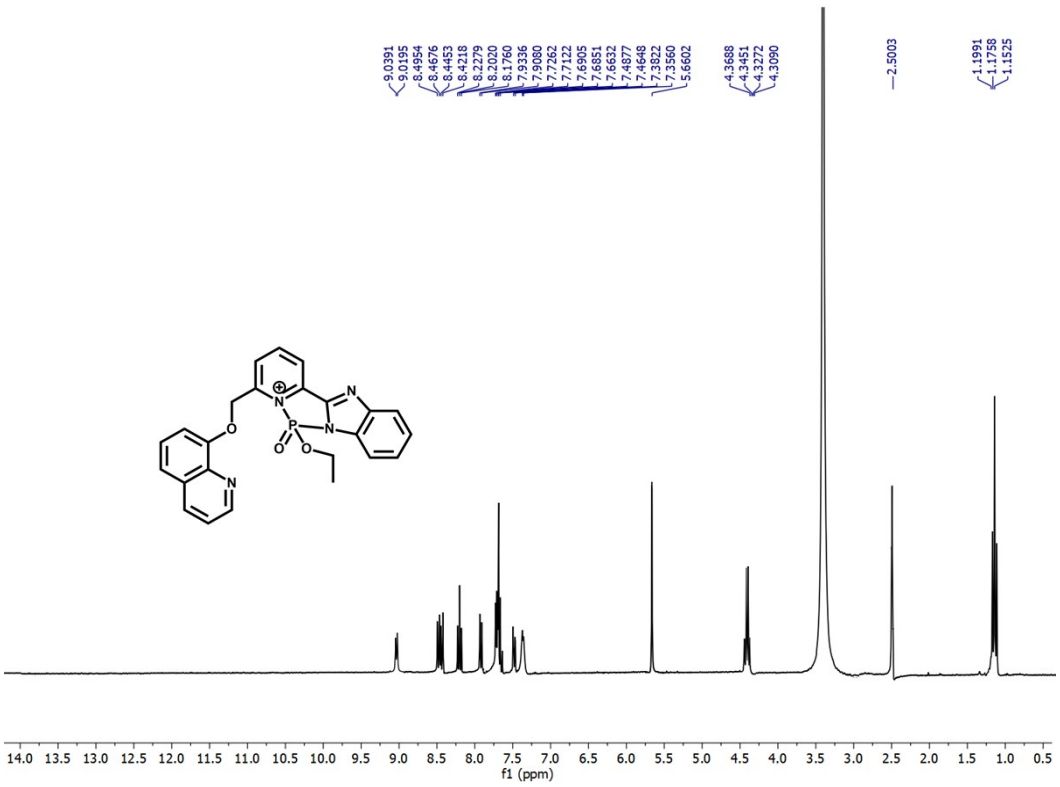

Fig.S5. ^{1}H NMR (300 MHz) spectrum of the adduct BIPQ-DCP in DMSO-d_6

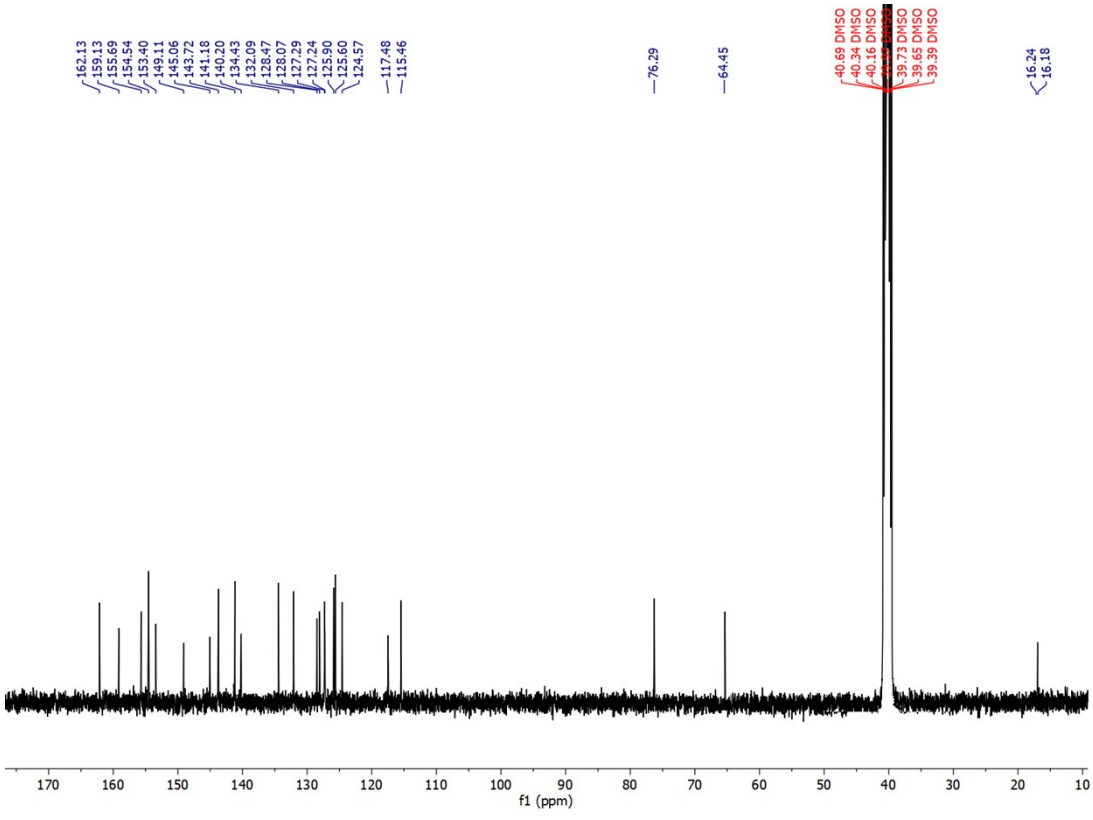

Fig. S6: ^{13}C NMR (75 MHz) spectrum of BIPQ-DCP adduct in DMSO-d_6

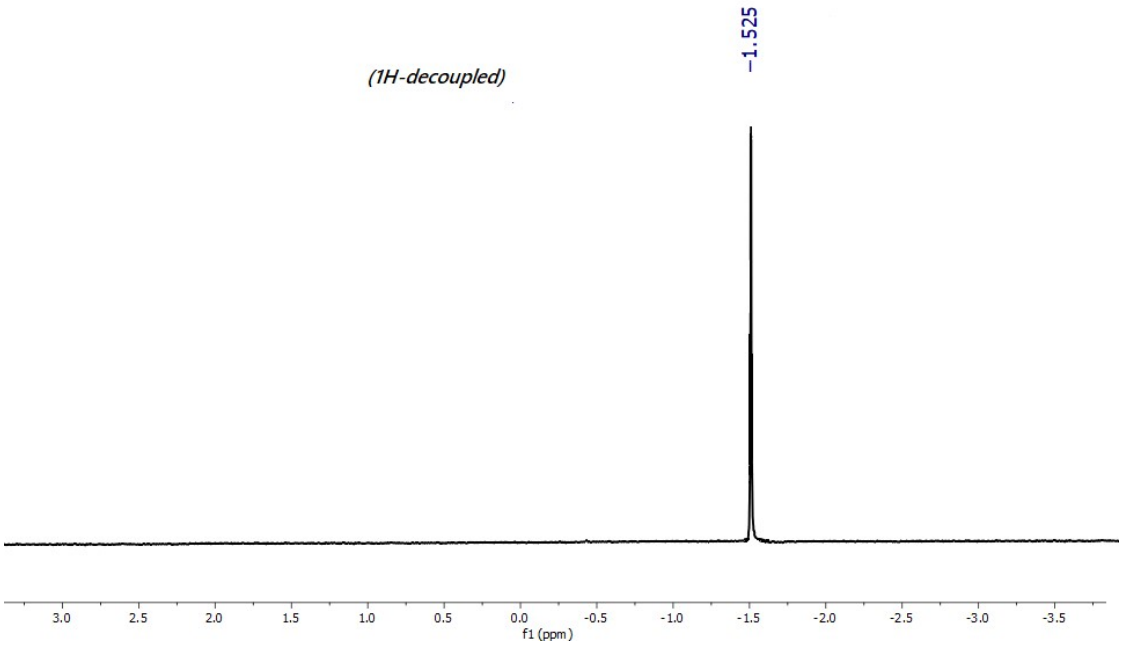

Fig. S7. ^{31}P NMR (100 MHz) spectrum of the adduct BIPQ-DCP in $CDCl_3$

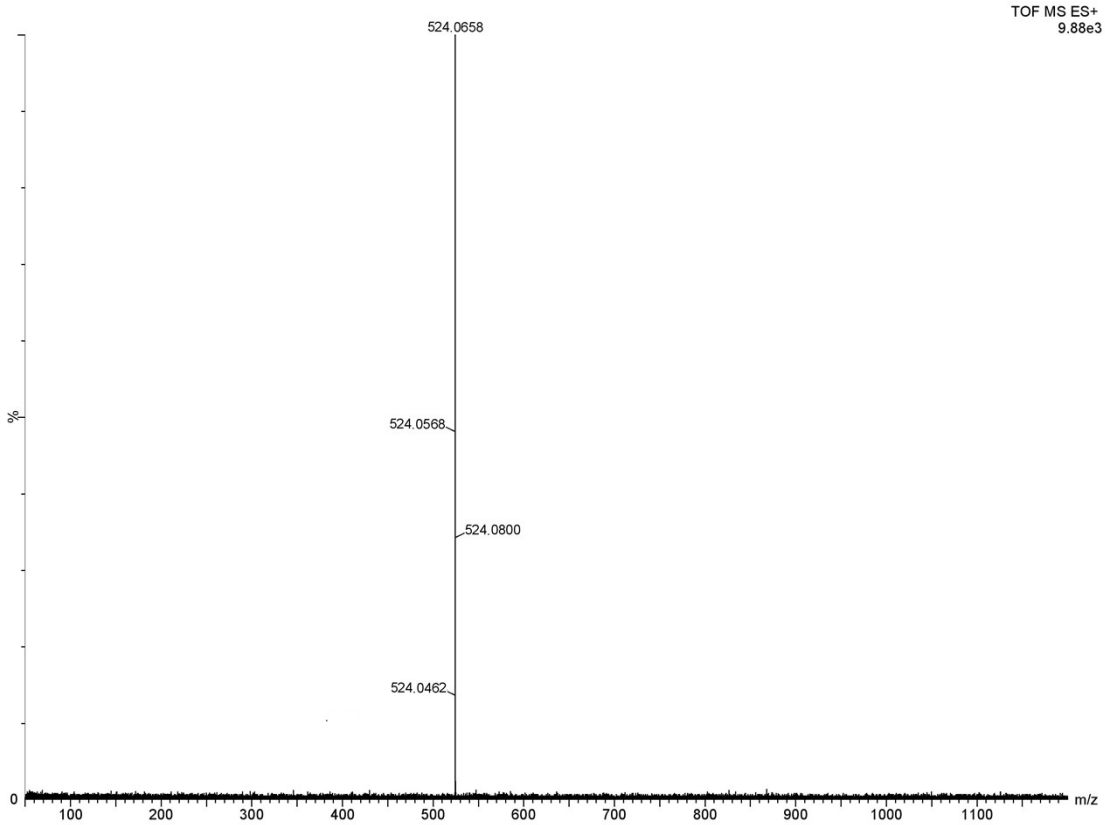

Fig. S8. HRMS of BIPQ-DCP product

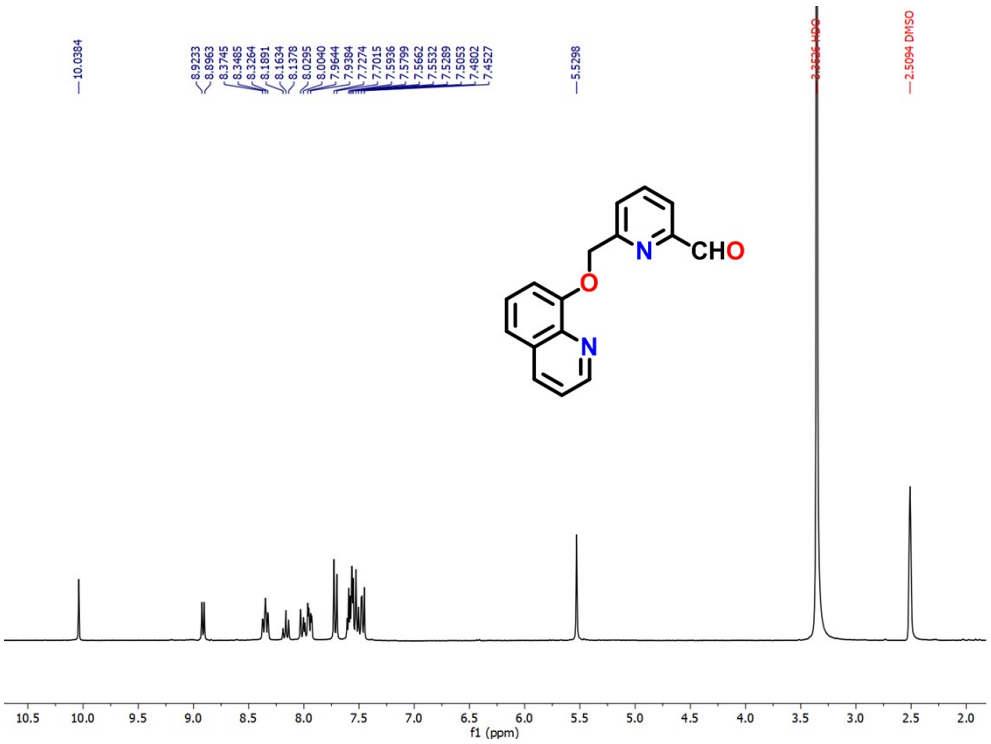

Fig. S9. ^{1}H NMR (300 MHz) spectrum of 6-((quinolin-8-yloxy)methyl)picolinaldehyde in DMSO-d_6

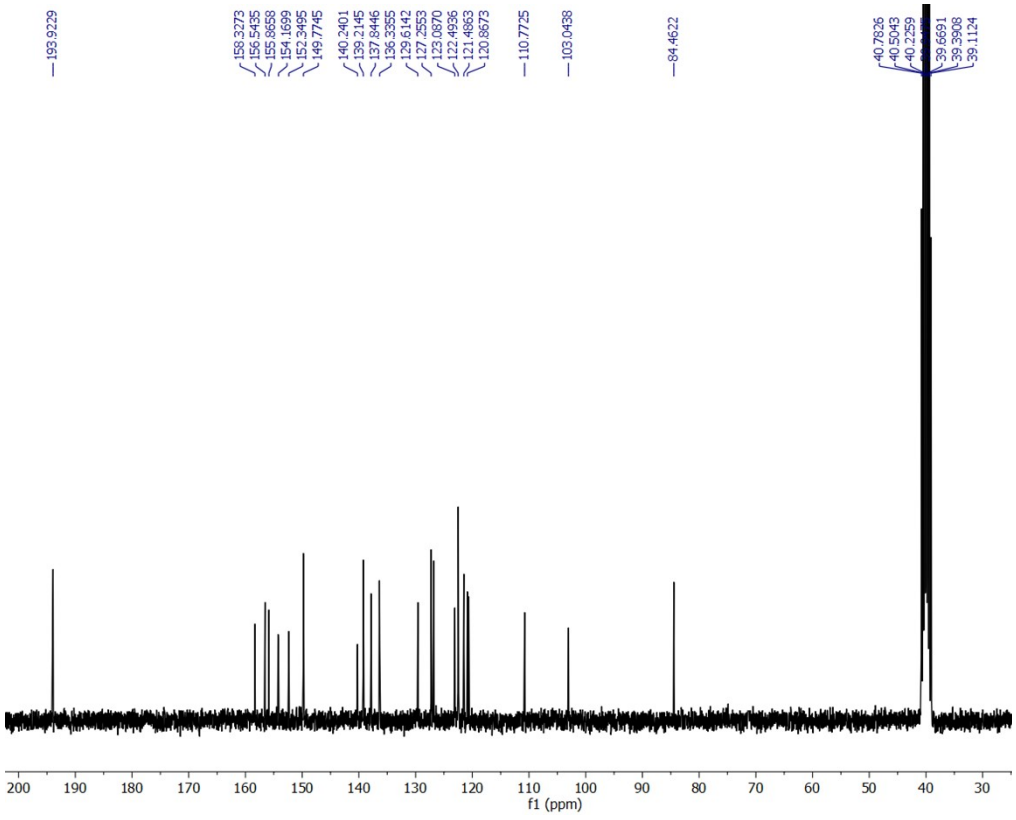

Fig. S10. ^{13}C NMR (75 MHz) spectrum of 6-((quinolin-8-yloxy)methyl)picolinaldehyde in DMSO-d_6

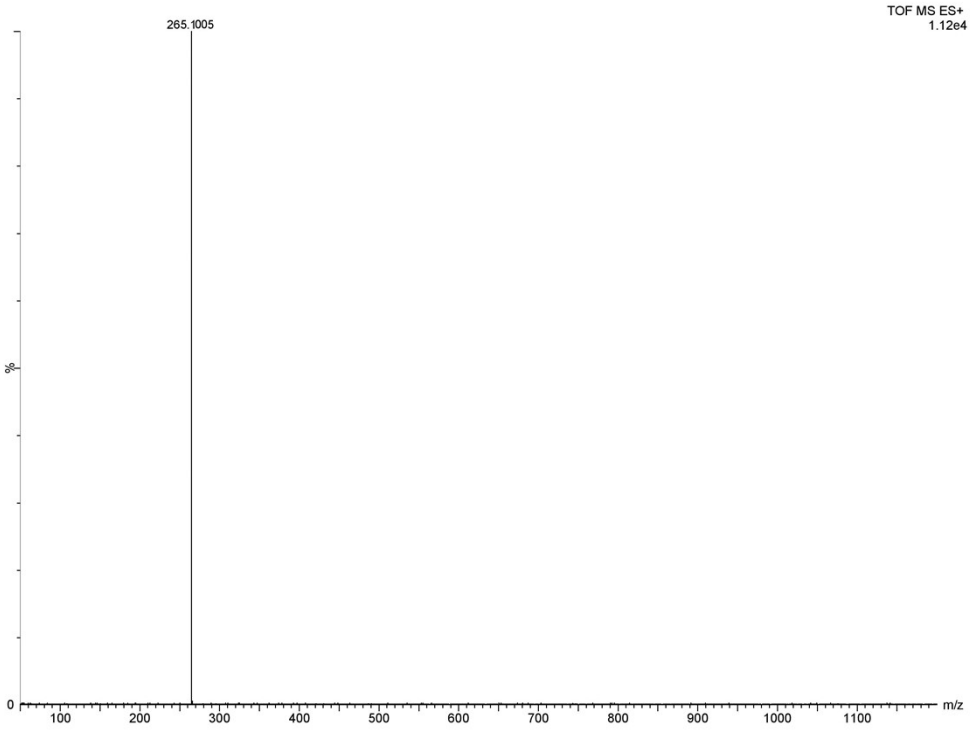

Fig. S11. HRMS of 6-((quinolin-8-yloxy)methyl)picolinaldehyde

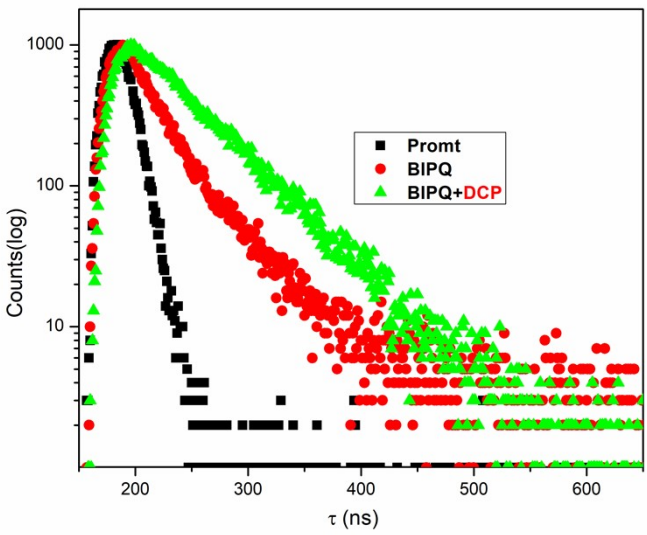

Fig. S12. Lifetime decay profile of BIPQ and BIPQ-DCP

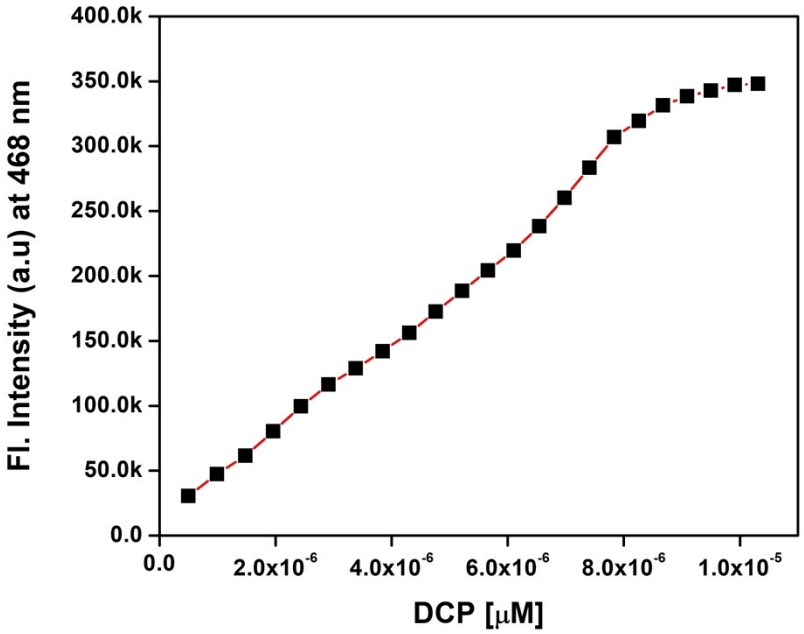

Fig. S13. Mole ratio plot of BIPQ for DCP

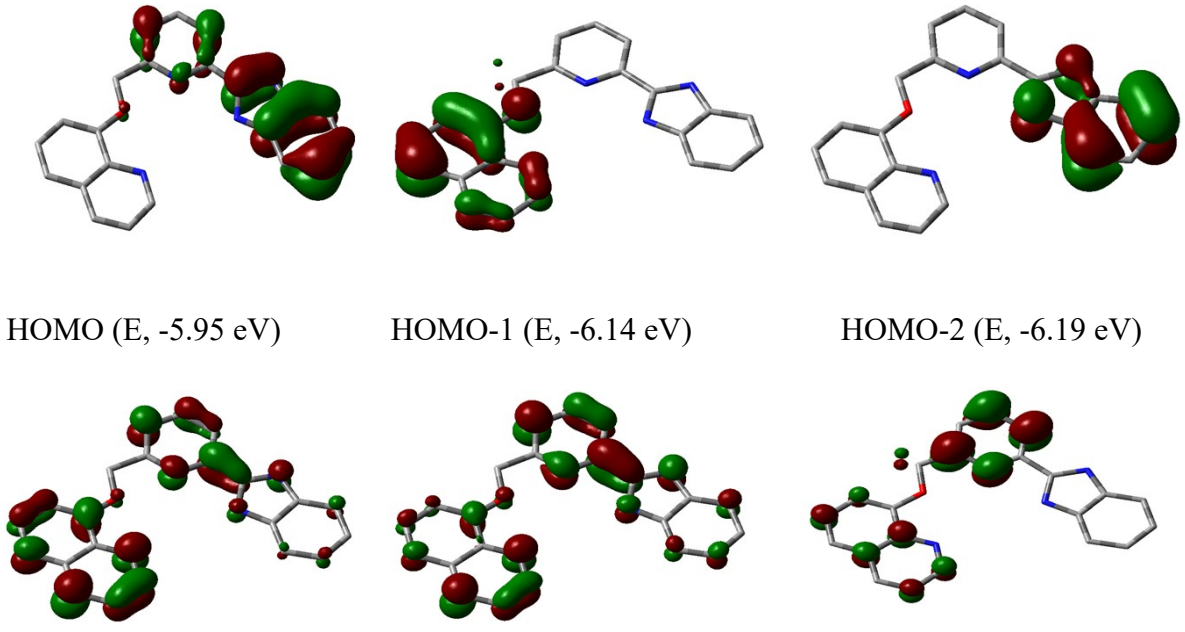

HOMO (E, -5.95 eV) HOMO-1 (E, -6.14 eV) HOMO-2 (E, -6.19 eV)

LUMO (E, -1.75 eV) LUMO+1 (E, -1.65 eV) LUMO+2 (E, -1.02 eV)

Fig. S14. Contour plots of selected molecular orbitals of receptor BIPQ

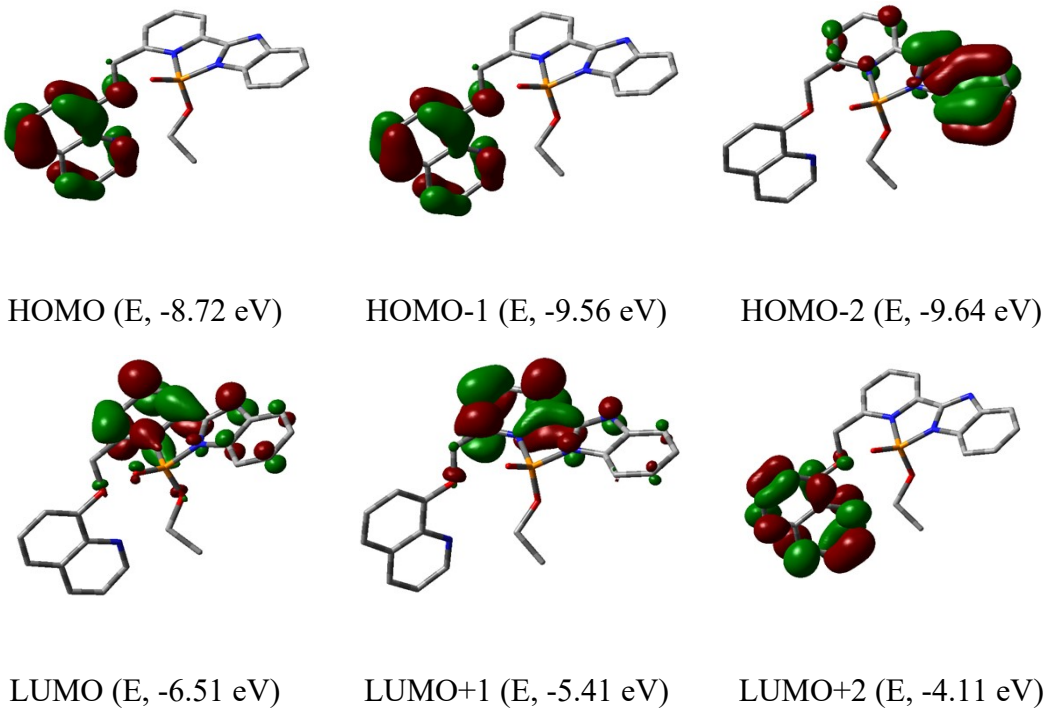

Fig. S15. Contour plots of selected molecular orbitals of BIPQ-DCP adduct

Determination of Quantum yield

For measurement of the quantum yields of BIPQ and the adduct BIPQ-DCP, we recorded the absorbance of the compounds in $CHCl_3$ solution. The emission spectra were recorded using the maximal excitation wavelengths and the integrated areas of the fluorescence-corrected spectra were measured. The quantum yields were then calculated by comparison with coumarin 153 (Φs= 0.544 in $CHCl_3$) as reference using the following equation:

$$\mathbf{\Phi_x = \Phi_s} \times \left(\frac{I_x}{I_s}\right) \times \left(\frac{A_s}{A_x}\right) \times \left(\frac{n_x}{n_s}\right)^2$$

Where, x & s indicate the unknown and standard solution respectively, Φ is the quantum yield, I is the integrated area under the fluorescence spectra, A is the absorbance and n is the refractive index of the solvent. We calculated the quantum yields of BIPQ and BIPQ-DCP using the above equation and the values are 0.21 and 0.35, respectively.

Table S1: Fluorescence lifetimes, quantum yields and radiative and non-radiative rate constants

$CHCl_3$ (solvent)	Quantum yield *(φ)*	τ (ns)	k_r ($10^8 \times s^{-1}$)	k_{nr} ($10^8 \times s^{-1}$)
BIPQ	0.21	1.71	1.228	4.619
BIPQ-DCP	0.35	2.31	1.515	2.814

Table S2. Vertical electronic transitions of BIPQ and BIPQ-DCP adduct calculated by TDDFT/CPCM method

Compds.	λ (nm)	E (eV)	Osc. Strength (f)	Key excitations
BIPQ	327.07	3.7907	0.2264	(86%)HOMO→LUMO
	317.76	3.9018	0.1604	(73%)HOMO→LUMO+1
	316.42	3.9184	0.4604	(92%)HOMO-1→LUMO
	236.65	5.2391	0.1650	(65%)HOMO-2→LUMO+3
	236.58	5.2406	0.3821	(30%)HOMO-3→LUMO+1
				(29%)HOMO-2→LUMO+3
	234.94	5.2772	0.3931	(35%)HOMO-6→LUMO
	208.88	5.9357	0.1484	(45%)HOMO-8→LUMO+1
BIPQ-DCP	568.57	2.1806	0.0184	(99%)HOMO→LUMO
	425.72	2.9123	0.3260	(33%)HOMO-2→LUMO
				(66%)HOMO-1→LUMO
	417.74	2.9680	0.1445	(65%)HOMO-2→LUMO
				(33%)HOMO-1→LUMO
	310.00	3.9995	0.1738	(97%)HOMO-1→LUMO+1
	309.11	4.0110	0.1178	(95%)HOMO→LUMO+2
	259.50	4.7777	0.1252	(91%)HOMO-7→LUMO
	232.98	5.3217	0.1931	(75%)HOMO-4→LUMO+3
	232.14	5.3409	0.6233	(32%)HOMO-3→LUMO+2

(29%)HOMO→LUMO+3

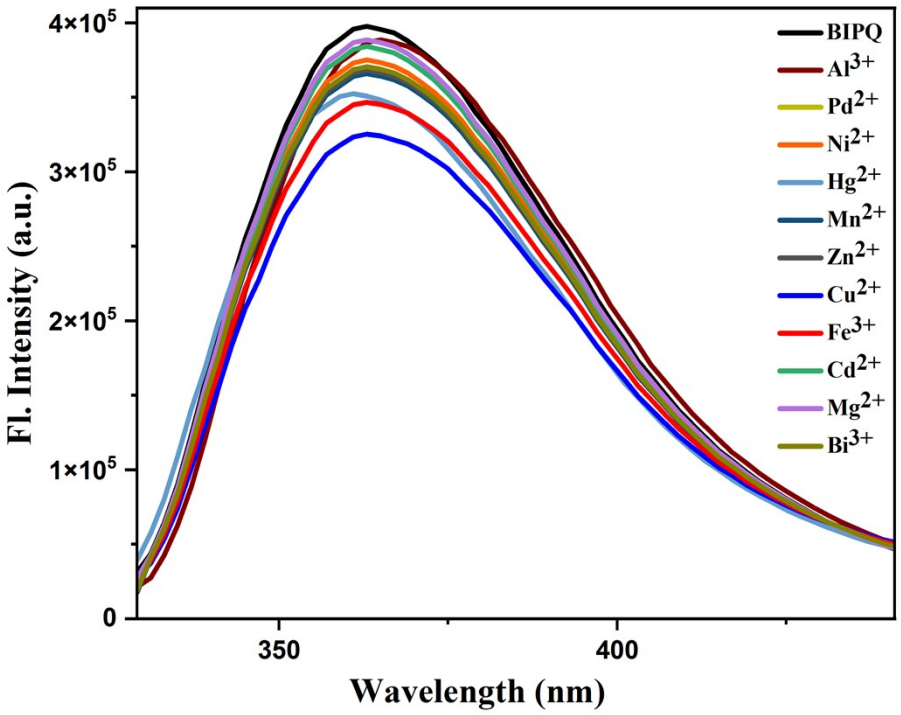

Fig. S16. Change in emission spectra of BIPQ (10 μM) in presence of various metal ions (20 μM) in $CHCl_3$

Table S3. Comparison of the present receptor (BIPQ) with the some reported receptors for the selective detection of DCP

Receptor	Solvent system	Detection limit	Reference
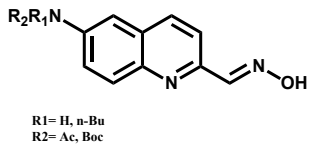 R1= H, n-Bu R2= Ac, Boc	CH_3CN	21 $\times 10^{-9}$ M	[1]
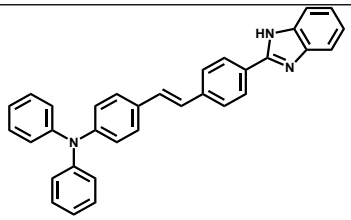	THF/H_2O (4/1, v/v)	8.45×10^{-8} M	[2]

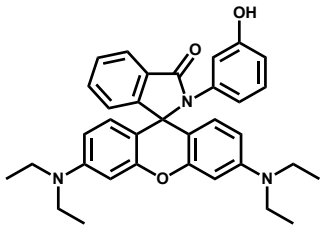	H_2O-CH_3CN (10:1, v/v)	5.6×10^{-9} M	. [3]
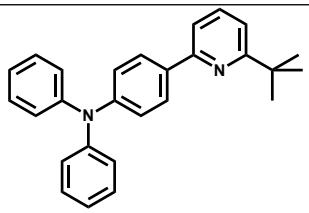	THF	1.5×10^{-8} M	[4]
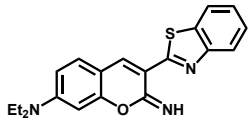	DMF (Fluorescence turn off chemosensor)	0.065 μM	. [5]
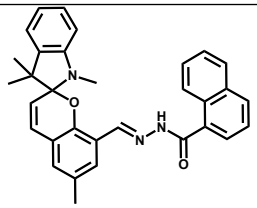	CH_3CN/H_2O (1/1, v/v)	2.1×10^{-8} M	[6]
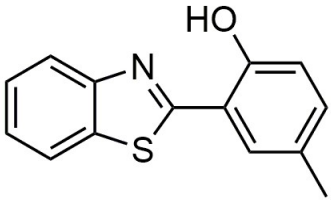	CH_3CN	0.186 μM	. [7]
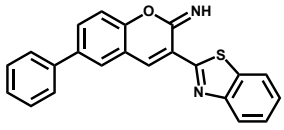	CH_3CN/H_2O (1/1, v/v)	15.8×10^{-9} M	[8]

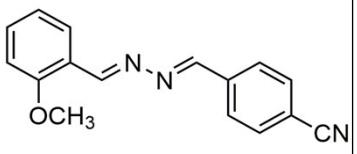	CH_3CN	9.86 nM	[9]
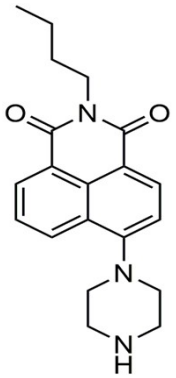	DMF	5.5 nM	[10]
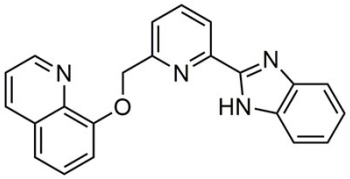	$CHCl_3$	$1.21x10^{-8}$ M	**This work**

References

[1] Y. Cai, C. Li and Q. Song, *J. Mater. Chem. C*, 2017, **5**, 7337-7343

[2] K. Aich, S. Das, S. Gharami, L. Patra and T. K. Mondal, *New J. Chem.*, 2017, **41**, 12562-12568

[3] H. S. Sarkar, A. Ghosh, S. Das, P. K. Maiti, S. Maitra, S. Mandal and P. Sahoo, *Sci Rep.*, 2018, **8**, 3402

[4] J. Yao, Y. Fu, W. Xu, T. Fan, Y. Gao, Q. He, D. Zhu, H. Cao and J. Cheng, *Anal. Chem.*, 2016, **88**, 2497-2501

[5] M. S. J. Khan, Y. W. Wang, M. O. Senge and Y. Peng, *J. Hazard. Mater.*, 2018, **342**, 10-19.

[6] S. Goswami, S. Das, and K. Aich, *RSC Adv.*, 2015**, 5**, 28996-29001

[7] X. Hu, H. Zeng, T. Chen. H. Yuan and L. Zeng, Sens. Actuators B Chem., 2020, **319**, 128282.

[8] L. Patra, P. Ghosh, S. Das, S. Gharami, N. Murmu and T. K. Mondal, *J. Photo. Photobiol. A. Chem.*, 2020, **388**, 112188.
[9] R. Suhasini, R. Karpagam, K. Thirumoorthy and V. Thiagaranjan, *Spectro. Acta, Mol. Bio. Spec.*, 2021, **263**, 120206.
[10] H. Xu, H. Zhang, L. Zhao, C. Peng, G. Liu and T. Cheng, *New J. Chem.*, 2020, **44**, 10713.